



UNIVERSITY OF LEEDS

This is a repository copy of *Comparing the Deployment of Non-Ionic Polymers to Dewater Organic/ Inorganic Radwaste Suspensions: Learning from Experience-23549*.

White Rose Research Online URL for this paper:

<https://eprints.whiterose.ac.uk/197260/>

Version: Accepted Version

Proceedings Paper:

Lockwood, A.P.G., Bell, M, Rumney, R.L.J. orcid.org/0000-0001-5160-4363 et al. (3 more authors) (2024) Comparing the Deployment of Non-Ionic Polymers to Dewater Organic/ Inorganic Radwaste Suspensions: Learning from Experience-23549. In: WM2023 Conference Proceedings. Waste Management Symposia WM2023, 26 Feb - 02 Mar 2023, Phoenix, USA. WM Symposia .

Reuse

Items deposited in White Rose Research Online are protected by copyright, with all rights reserved unless indicated otherwise. They may be downloaded and/or printed for private study, or other acts as permitted by national copyright laws. The publisher or other rights holders may allow further reproduction and re-use of the full text version. This is indicated by the licence information on the White Rose Research Online record for the item.

Takedown

If you consider content in White Rose Research Online to be in breach of UK law, please notify us by emailing eprints@whiterose.ac.uk including the URL of the record and the reason for the withdrawal request.



eprints@whiterose.ac.uk
<https://eprints.whiterose.ac.uk/>

Comparing the Deployment of Non-Ionic Polymers to Dewater Organic/ Inorganic Radwaste Suspensions: Learning from Experience-23549

Alexander P. G. Lockwood^{}, Michael Bell^{*}, R. L. Jacob Rumney^{**}, David Harbottle^{**}, Martyn G. Barnes^{*} and Timothy N. Hunter^{**}.*

**Particles with Fluids Centre of Expertise, Sellafield Ltd. Hinton House, Birchwood, UK, WA3 6GR*

***School of Chemical and Process Engineering, University of Leeds, Leeds, LS2 9JT*

1. ABSTRACT

Due to the high degree of scrutiny and regulation in the nuclear industry, standardization of chemical additives reduces the need for multiple holistic assessments. These include the impact on the operation of in sequence processing plants and long-term stability in a geological disposal facility. A non-ionic polyacrylamide commercial settling aid has been suggested to remove Magnox fuel degradation product colloidal challenges from UK ion exchange processes. This decision involved research and development stages which tested multiple settling aids and through analysis of settling performance and degradation products. As a result, the polyacrylamide was selected as the best available technique. It was then suggested that polyacrylamide could potentially be deployed to improve the clarification of liquors from pond water which has held a range of fuel types and debris. However, even though pond water is at a lower pH and consists of organic contaminants from algal blooms, the efficacy of the polyacrylamide was found to be superior in settling organic laden wastes. These wastes were more complex composition than the Magnox based material, where polyacrylamide was selected through experimental trials specific to Magnox based particles. In this paper the surface properties and floc structures of the two waste types are compared and the most influential properties on settling are scrutinized. Then learning from experience is discussed to identify how the Magnox settling aids programme could be used to accelerate the technology readiness level of deploying settling aids to tackle slow settling and colloidal challenges in other waste streams at the Sellafield site. Due to high levels of regulation, standardization of chemical reagents whose lifetime process and environmental impact from deployment to disposal have been reviewed is a powerful tool if the reagent can be applied to other processes. In this paper, the performance of a tailor selected non-ionic polymer to flocculate Magnox waste was compared to using the same polymer to flocculate a different organic laden waste with differing water chemistry. Key analyses were identified and learning from experience is discussed to accelerate the identification of other wastes which can also be targeted by the same polymer accelerating delivery.

2. INTRODUCTION

Standardization has been a driving factor in nuclear new build design, as it will decrease cost through repeatable construction and provide a pool of subject matter experts across the industry to troubleshoot issues that arise (Mignacca et al., 2020). The same concept can be applied to aspects of nuclear decommissioning, especially when it comes to compatible reagents with the

range of complex interlocked processes found in nuclear reprocessing and waste treatment facilities. Sellafield Ltd. is a complex and congested nuclear licensed site that hosts a range of facilities connected to multiple, often in series and in parallel, donor plants (Arnold, 2007). This means that small changes in process chemistry upstream can have propagating impacts on radionuclide abatement potential of critical enablers such as the site ion exchange effluent plant (SIXEP) or the enhanced actinide removal plant (EARP) (Dyer et al., 2018). It is being recognized that due to the challenges of physical properties arising from legacy waste deposits (rheology, crystallization etc.) that behavioral modifiers may need to be deployed to improve the post operational cleanout (POCO) and waste retrieval processes during decommissioning of the Sellafield site (Hastings et al., 2007). Therefore, understanding the impacts of these reagents upstream through to downstream is a critical and often rate determining step of the reagents deployment. Furthermore, the reagent must be compatible with immobilization and encapsulation techniques to promote stability in a geological disposal facility (GDF). Though with advances in thermal treatment options of Magnox containing sludges this could completely circumvent the issues through organic component combustion (Barlow et al., 2021).

Upstream of SIXEP is the Magnox swarf storage silo (MSSS) which feeds to the effluent distribution tank (EDT) along with the first-generation Magnox storage pond (FGMSP) prior to SIXEP and ultimately sea discharge (Fig. 1). Due to the process conditions in the MSSS, the corrosion and precipitation of Magnox alloy (~0.8% Al, 50 ppm Be) (Hallam et al., 2016) and precipitation of $Mg(OH)_2$ species may lead to the production of a morphology referred to as 'beta star' (Maher et al., 2016). This colloidal material provides a challenge to the downstream SIXEP facility as they have been found to pass through sand bed filters unabated, they can potentially impact ion exchange beds in SIXEP and have been found to be vectors for the transport of americium and plutonium through SIXEP (Maher et al., 2014). There is little maneuverability to address this challenge in the plants current configuration, where dilution by blending fuel handling plant (FHP) liquor to reduce particle concentrations and discharge directly to the bulk storage tanks (BSTs) would potentially impact future ion exchange capacity (Fig. 1). In response to the potential challenge to SIXEP, research was commissioned to identify aggregation agents to improve the settling characteristics of beta star colloidal material. The work identified the presence of beta star in process streams, produced a beta star simulant and screened for an effective aggregation agent based on performance and potential downstream impacts. A commercial homopolymer of polyacrylamide was selected as an aggregation reagent as the polymer successfully flocculated and settled the beta star and is suspected to have the least potential impact to downstream processes/GDF due to the speciation of its radiolytic and alkali hydrolysis degradation products, though further work is required on microbial catabolism of polyacrylamide (Levitt, et al. 2011; Nyssola and Ahlegren 2019).

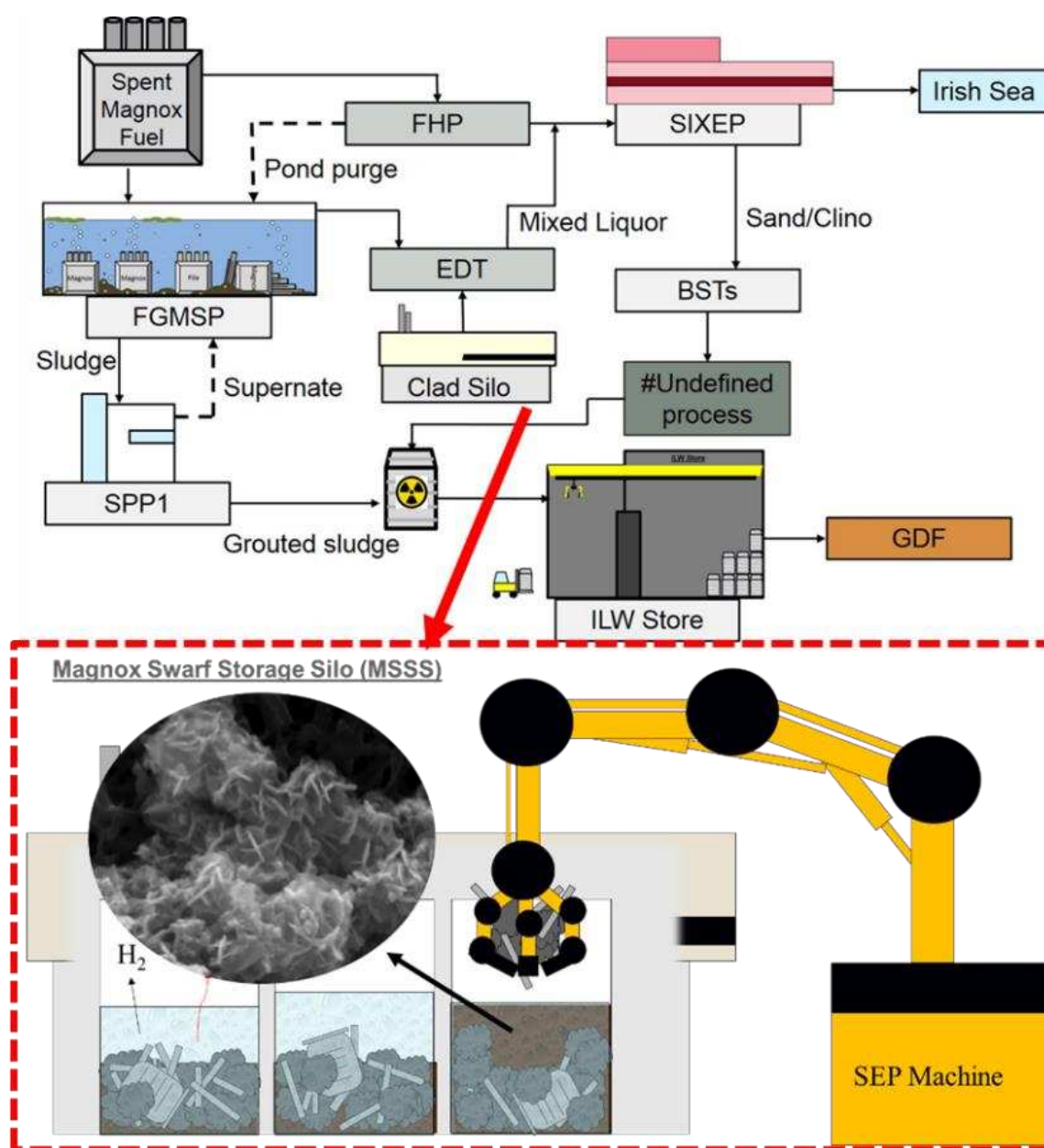


Figure 1: Flowsheet of donor plants feeding into the site ion exchange effluent plant (SIXEP): first generation Magnox storage pond (FGMSP), fuel handling plant (FHP), Effluent distribution tank (EDT), sludge packaging plant (SPP1), intermediate level waste (ILW) store, geological disposal facility, bulk storage tanks (BSTs), Magnox swarf storage silo (clad silo) and silo emptying plant (SEP).

The first of the legacy spent nuclear fuel ponds at Sellafield was built to store Pile fuel from the Pile reactors commissioned to aid the nuclear deterrent programme (Arnold, 2007). Due to the material section for the Pile fuel, they did not corrode to the extent of Magnox fuel rods thus not require pH adjustment through caustic to 10-11 unlike FGMSP. This has however led to issues with algal blooms, in addition to other contaminants from windblown debris and bird guano, the remaining sludge is a composite of inorganic silts, sands and clays and an organic fraction found to be bound through extracellular polymeric substances from diatoms (Gregson et al., 2011; Hastings et al., 2007; Jackson et al., 2014; Lockwood et al., 2022; Woodall et al., 2021). These composite properties result in the sludge behaving in two phases, a fast-settling

α -phase and a slow settling turbid β -phase (Lockwood et al., 2022). As FLOPAM FA 920 SEP has been screened for compatibility with downstream processes and long-term stability in a GDF, the direct deployment of the polymer to treat the inorganic/organic composite sludge β -phase would accelerate deployment significantly and reduce research and development costs.

In this paper, the experimental results of the flocculation of corroded Magnox sludge (CMS) and a Pile fuel Storage Pond sludge (PFSPS) test material were compared to each other and literature to identify important properties and critical variables to be understood before deployment. Additionally, Sellafield and other international nuclear waste management sites has a variety of sludge and slurry-based wastes such as clinoptilolite and storage tank heels which require mobilization before retrieval processes can segregate this particulate waste (Prajitno et al., 2021). Remobilization potentially can resuspend slow settling or colloidal material and threaten downstream processes which could be treated with the same or similar flocculation strategies (Hastings et al., 2007). This paper identifies key variables to understand, accelerating deployment in other areas by learning from experience.

3. MATERIALS AND METHODOLOGY

3.1. Test Materials

3.1.1. Corroded Magnox Sludge

Corroded Magnox sludge (CMS) was provided by the National Nuclear Laboratory (NNL). The CMS was produced from the extensive corrosion of Magnox AL 80 (assumed to be the predominant alloy in various legacy facilities). The CMS was corroded for up to 3 months at a temperature of 50 to 60°C with an electrolyte concentration of 300 ppm NaCl. This corroded mixture is processed through a 200 μm sieve before a settling stage, the sludge is then concentrated through a centrifuge (4000 rpm) and processed into 220 L drums. This stock sludge was used for all flocculation experiments and diluted accordingly to achieve target concentrations. All CMS suspensions were adjusted to pH 11.5 using NaOH ($\geq 99\%$; Sigma Aldrich, USA) to replicate plant conditions.

3.1.2. Pile Fuel Storage Pond Sludge

Experiments were carried out using a Pile fuel storage pond sludge (PSPS) test material sourced by Barron Ltd. (Appleby-in-Westmorland, UK) called Appleby sludge. The sludge, previously used by the authors (Lockwood et al., 2022) was derived from a pond situated at an old dairy site in Appleby owned by Barron Ltd., which is an open-air environment that has accumulated silt, organic matter, and wind-blown debris over the course of a number of years. The material has previously been selected as a radwaste test material by Sellafield Ltd., where it has been proposed that the Appleby sludge surface chemistry is likely representative of pile fuel storage pond sludge.

3.1.3. Reagents

As used in the authors previous work (Lockwood et al., 2022) FLOPAM FA 920 SEP, manufactured by SNF Ltd. (Wakefield, UK) was selected as a flocculation agent. FLOPAM FA 920 SEP, referred to hereon as 'FLOPAM' is a water-soluble polyacrylamide flocculation agent with a molecular weight of $5 \times 10^6 \text{ g}\cdot\text{mol}^{-1}$ - $15 \times 10^6 \text{ g}\cdot\text{mol}^{-1}$. Stock solutions of FLOPAM were prepared in concentrations of 1000 and 10000 ppm in deionized water at 25°C and stirred with a magnetic stirrer bar at 250 rpm for a minimum of 3 hours based on manufacturer instructions. Sodium chloride (NaCl) ($\geq 99\%$; Sigma Aldrich, USA) was used as an electrolyte background in flocculation of CMS using FLOPAM.

3.2. Experimental Methodology

Due to the differences in available volumes of the two test materials, experimental approaches differed between research portfolios. The main difference being that PFSPS tests were completed at lower volumes due to the availability of material. The experiments conducted are listed below in Table 1 and methodologies detailed further in this section.

Table 1: Experiment array and comparison for the Pile fuel storage pond and corroded Magnox sludge test materials.

Experiment	CMS	PFSPS
Test Material characterisation	Scanning electron microscopy and zeta potential	Scanning electron microscopy and zeta potential
Flocculation using FLOPAM	1 L	200 mL
Floc Size Characterisation	Focus beam reflectance measurement (<i>in situ</i>)	Single element automated microscopy (<i>ex situ</i>)
Polymer adsorption	Differential total organic carbon	Differential total organic carbon
Efficacy of polymer addition	Zonal settling rate and turbidity measurements	Zonal settling rate and turbidity measurements
Impact of solids content	Settling rate measurements	Material restrictions
Impact of electrolyte	Settling rate measurements, turbidity, adsorption, floc size measurements	Material restrictions
Impact of Shear rate and time	Completed using FBRM <i>in situ</i>	Material restrictions: prevented loading of FBRM with sufficient submergence.

3.2.1. Test Material Characterization

Dried CMS and PFSPS sludge samples were characterized using scanning electron microscopy (SEM) (Hitachi SU8230 scanning electron microscope; Hitachi Hightech) after being coat in 10 nm thickness layers of iridium to investigate the structure and morphology of the particles. zeta-potential was identified via electrophoresis using a Zetasizer Advance (Malvern Panalytical, UK).

3.2.2. Flocculation of Test Materials

The sludge test materials were diluted as required (250 mL and 1 L for PFSPS and CMS respectively) transferred to a 4 L baffled tank used in previous work (Lockwood et al. 2021a; Lockwood et al., 2022) equipped with an overhead stirrer and a 48.2 mm 60° pitch blade impeller and was mixed at a rate of 200 rpm (PFSPS) or 300 rpm (CMS) to ensure that particulates were fully suspended. Flocculant was transferred via micropipette from the 1000 and 10000 ppm stock solutions to achieve concentration ranges of 1.25-100 ppm and 12-300 ppm of FLOPAM in the bulk solution for PFSPS and CMS respectively. The mixture was then left to flocculate for 5 minutes before being transferred to a 250 mL or 1 L (PFSP and CMS respectively) measuring cylinder for multiple analysis purposes.

3.2.3. Floc Size Characterization

CMS was characterized *in situ* using focus beam reflectance measurement (FBRM) model PI-14/206 (Mettler-Toledo, USA). CMS was added in a concentration range of 0.5 to 1.25 vol.% and flocculated with FLOPAM after 5 minutes of agitation at 300 rpm. *The in situ floc growth kinetics were recorded by using an FBRM in macro-mode with a laser scanning speed of 8 m.s⁻¹.* the probe was placed 3 cm from the base of the reactor vessel at a 45° angle to ensure representative flow across the measurement window as per our previous work (Lockwood et al. 2021). Measurements were taken every 15 seconds for 15 minutes immediately after addition of the FLOPAM. The volume weighted mean chord length ($d_{4,3}$) was then recorded as a function of time. The bulk stock of PFSPS was probed *in situ* with FBRM to determine the chord length distribution of the fast-settling $\alpha\beta$ -phase and slow settling β -phases by separating after settling for 1 hour in 1 L volumes which were then remixed and added back to the stock of PFSPS to conserve material. Because of the lower volume of available PFSPS, the flocs were sized using a Morphologi G3 (Malvern Panalytical Ltd.) automated single element microscope. *Ex situ* samples were taken from the flocculation vessel after 5 minutes of agitation at 200 rpm using a wide bore pipette and placed upon to 3 microscope slides.

3.2.4. Polymer Adsorption

The supernatant total organic carbon (TOC) concentration of flocculated and settling CMS and PFSPS was compared to a supernatant water sample without polymer establishing a TOC background to differentially determine the adsorption of FLOPAM onto the particles as FLOPAM concentration is linearly proportional to increases in carbon concentration. The TOC analysis was completed using a Jena Multi N/C 2100 (Analytik Jena, Germany).

3.2.5. Efficacy of Polymer Addition

To measure the efficacy of the polymer additions to the CMS and PFPS, two metrics were used to compare performance, the zonal settling rate and the supernatant turbidity which was determined using a TN-100 turbidity meter (Eutech Instruments, UK). The zonal settling rate was determined using a 1 L measuring cylinder for the CMS and 250 mL measuring cylinder for the PFSPS which a calibrated adhesive measuring tape from which the zonal settling front could be tracked with time. Samples were taken at 5 cm below the air-water interface.

3.2.6. Efficacy of Polymer in the Presence of Electrolyte

Systems of 1.25 vol.% CMS were prepared with 200 ppm FLOPAM and increasing concentrations of NaCl as per Section 3.2.2 and the zonal settling rates were examined as per Section 3.2.5.

3.2.7. Efficacy of Polymer in the Presence of Shear

A 1.25 vol.% suspension was prepared with a 1 mM NaCl background and 200 ppm of FLOPAM as per Section 3.2.2. The system was analyzed *in situ* with FBRM using the methodology in Section 3.2.3. The difference being the variability of shear in the flocculation vessel, varying from 300 rpm to 50 rpm in a stepwise manner over a period 60 minutes. The shear rate was then instantaneously increased back to 300 rpm and then the stepwise decrease to 50 rpm was repeated for another 60 minutes reporting the volume weighted average chord length as a function of time.

4. RESULTS AND DISCUSSION

The structure differences between CMS and PFSPS were interrogated using SEM. A SEM image of PFSPS is shown in Fig. 2A and CMS in Fig. 2B. There is a marked difference between the samples as seen by the compaction of the nano-crystalline platelet structure which forms the aggregates. Fig. 2A shows a tightly compact structure, where the constituent primary particles of PFSPS have a face-face agglomeration configuration, whereas the CMS (Fig. 2B) shows a less compact and more porous agglomerate structure with constituent platelets interacting via face-edge and face-face configurations. Additionally, there are complex surface phenomena occurring in the PFSPS sample, where the presence of pennate diatoms can be seen. Our previous work (Lockwood et al. 2022) probed this material with energy dispersive x-ray (EDX) analysis and found complex heterogenous surface sites comprising of inorganic and organic species with the presence of various oxides (calcium, magnesium, aluminum and silicon), indicating the presence of silts and clay species such as montmorillonite (Sabbagh et al., 2019) or chlorite (Koutsopoulou et al., 2010). In addition, the presence of pennate diatoms is associated with the excretion of extra-cellular polymeric substances which is known to bind silts of various compositions contributing to the composite nature of the material (Hope et al., 2020). Metal (hydr)oxide surface chemistry is complex, with $Mg(OH)_2$ test materials reported to have a self-buffering nature and a tendency to aggregate at their natural pH due to low surface potentials as well as a vulnerability to strong aggregation at low electrolyte concentrations (Lockwood et al., 2021b). Rapid agglomeration of $Mg(OH)_2$ results in complex aggregate structures with fractal dimensions in the order of 1.97 (Lockwood et al. 2021a; Lockwood et al., 2021b) compared to the natural state of PFSPS with a fractal dimension of 2.24 (Lockwood et al. 2022) indicating a more compact structure (de Martin et al. 2014). It is known that $\alpha-Al(OH)_3$ gibbsite, an analogous but more galvanically stable material structure to $Mg(OH)_2$ species such as brucite, possesses a similar pseudo-hexagonal crystalline platelet structure. Gibbsite basal plane and face speciation has a pH dependence regarding the surface potential due to differences between the face and edge crystal structures (Rosenqvist 2002; Wierenga et al. 1998), which could explain the combination of face-face and face-edge agglomerates if brucite consists of the same crystal structure plane differences shown in Fig. 2B.

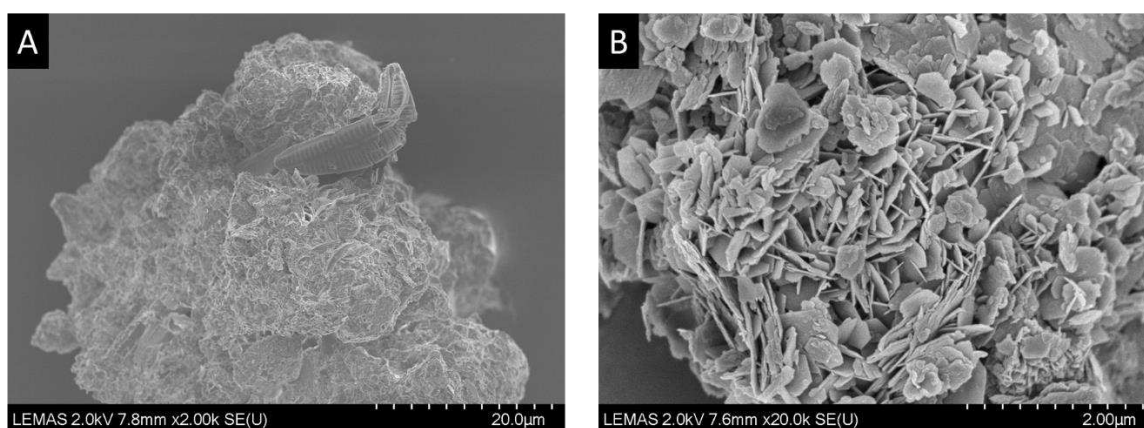


Figure 2: Scanning electron micrograph of A) Pile Fuel Storage Pond Sludge (PFSPS) and B) Corroded Magnox Sludge (CMS) simulants.

The affinity of FLOPAM® for the surfaces of CMS and PFSPS was assessed by measuring the total organic carbon concentrations of the supernatant liquor after the aggregates were

contacted and mixed with the FLOPAM solutions for 5 mins. For an assumed fixed molecular weight distribution, the carbon concentration is directly proportional to the concentration of FLOPAM. Figs. 3A and 3B show the total organic carbon concentrations for PFSPS and CMS respectively. This data is compared to the total organic carbon concentration of FLOPAM only without the addition of PFSPS or CMS. Fig. 3A shows a relatively stable total organic carbon concentration with increasing FLOPAM addition, whereas the control study (FLOPAM only) shows an increase in total organic carbon concentration with increasing FLOPAM addition. The stable total organic carbon concentration in supernatant qualitatively indicates a very high affinity of FLOPAM for the PFSPS surface as any FLOPAM in the bulk liquor would contribute to an increase in the total organic carbon concentration, indicating the majority must be associated with the solid PFSPS particulate phase. Conversely, Fig. 3B indicates that there is only a partial adsorption with increasing FLOPAM concentrations. As the FLOPAM concentration increases there is an increase in total carbon supernatant concentrations, though as concentration increases there is a relative decrease in the differential between the baseline and measured CMS supernatant sample, indicating an increase in the proportion of supernatant FLOPAM concentration. This result likely due to saturation of polymer on the CMS surface sterically preventing further adsorption (Gregory and Barany, 2011).

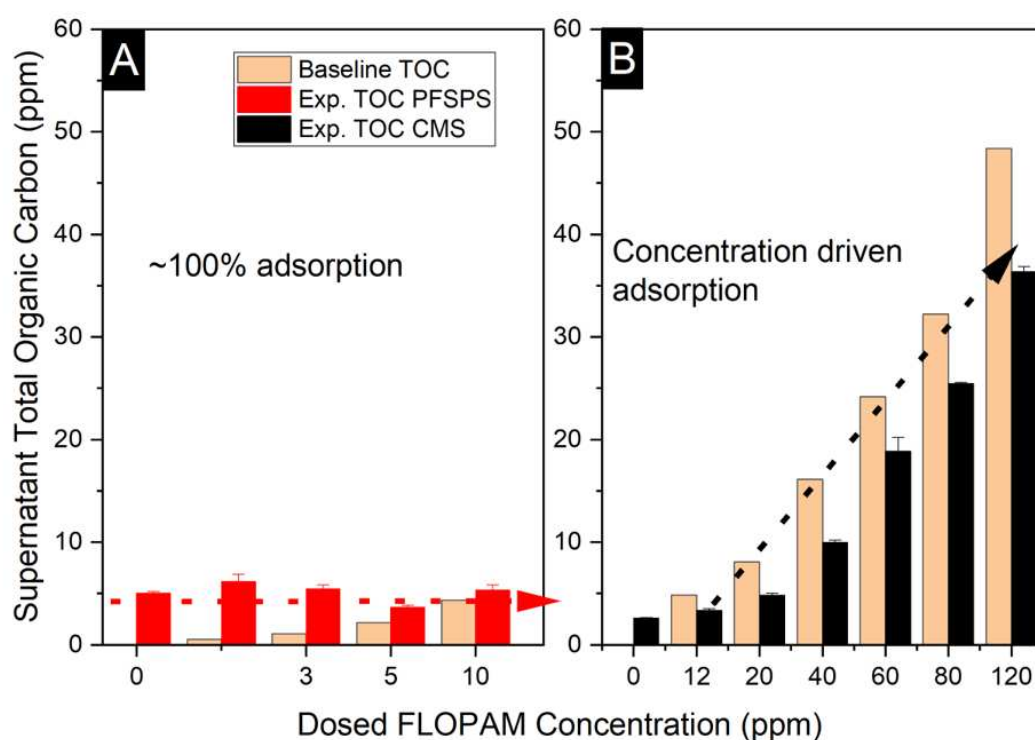


Figure 3: The supernatant total organic carbon concentration and baseline FLOPAM total organic carbon concentrations for A) PFSPS and B) CMS after mixing for 5 minutes at 200 rpm.

Adsorption affinity of polyacrylamide for a particle surface is a function of many factors including the particle surface charge (a function of the solution pH and electrolyte concentration), polymer conformation (a function of the electrolyte concentration), polymer molecular weight, and the polymer concentration in solution (Gregory and Barany, 2011). Molecular weight is crucial as adsorption involves the attachment of many polymer segments

to a particle surface, where each individual segment adsorption only requires a small reduction in free energy (~ 0.3 kT per segment) to compensate for the entropy loss that occurs when the whole polymer adsorbs from the solution to the particle surface (Gregory and Barany, 2011; O'Shea et al. 2010). For bridging flocculation mechanisms, the molecular weight for linear polymers informs the chain length. The polymer resultant loops and tails must be able to extend beyond the Debye layer (which provides the colloidal stability of particles) to attach to an adjacent particle to facilitate flocculation (Sung et al., 2018; Gregory and Barany, 2011). This is an important factor for industry to consider as commercial availability of the FLOPAM FA 920 SEP polymer cannot be credibly guaranteed for the duration of nuclear decommissioning timelines, however for this work, the molecular weight distribution is considered consistent.

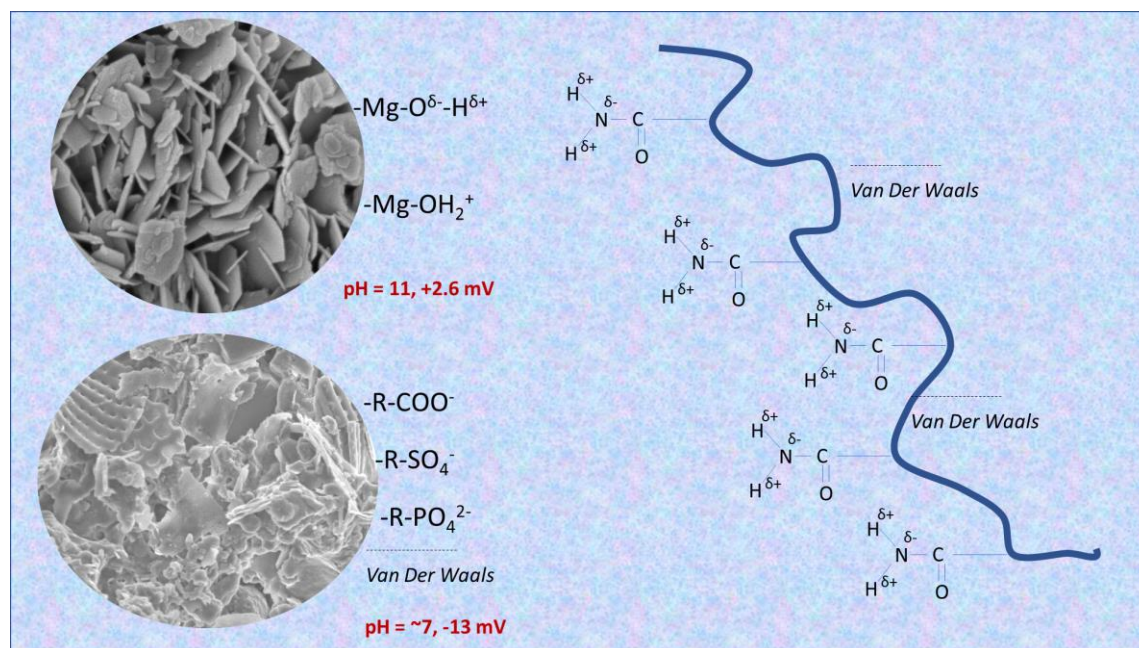


Figure 4: Diagram showing the corroded Magnox sludge (CMS) (top) and Pile fuel storage pond sludge (PFSPS) (bottom) surface speciation and adsorption mechanisms of FLOPAM FA 920 SEP polyacrylamide.

The heterogeneity of PFSPS indicates the presence of complex solution chemistry with full characterization in the electronic supplementary material of the authors previous work (Lockwood et al., 2022). The partial solubility and buffering of CMS in combination with the additional NaOH for pH adjustment indicates excess electrolyte presence (Lockwood et al., 2021a). Whilst it is impractical to compare the ionic strengths of the PFSPS and CMS liquors due to the uncertainty of non-additive contributions to polymer-particle interactions w.r.t. specific ion affects present in the heterogeneous PFSPS system (Gregory et al., 2022), the influence of Debye screening on the polymer functional groups and particle surfaces is not negligible.

Polyacrylamide has a resistance to coiling to the point of globule regarding amide functional group segment-segment repulsion screening preventing complete collapse, but the electrostatic interactions between the amide functional group dipole and surface species of the CMS and PFSPS will be affected to differing degrees (Ji et al., 2013). Furthermore, the low surface potential of the CMS from protonated and unprotonated hydroxyl surface groups may provide less electrostatic influence on the dielectric medium in addition to OH^- , Mg^{2+} and Na^+ electrical

double layer formation and surface charge screening (discussed further in Section 5). The greater magnitude of surface potential (-13 mV) of the PFSPS due to the presence of carboxyl, phosphate and sulphate groups associated with decaying algal matter (Roselet et al., 2015) provides greater electrostatic influence on the dielectric medium which would weakly attract the permeant dipole of the N-H bonds in the amide functional group of the polyacrylamide (see Fig. 4) to a greater degree (Nasser and James, 2006). Additionally, the near neutral pH of the PFSPS liquor would present a lower OH^- and associated metal cation concentrations reducing their contributions to Debye screening, alas the PFSPS complex solution chemistry may compensate for the basic ionic deficit (Lockwood et al., 2022). Ultimately, the PFSPS provides a stronger electrostatic influence on the dielectric medium to attract the amide functional group permanent dipole to form hydrogen bonds on the PFSPS surface compared to CMS (-13 mV and 2.6 mV respectively). Though this electrostatic influence is likely negligible compared to random Brownian motion and mixing contacting the polymer with the particle surface. A final consideration is the presence of organic decaying material. The long chain organics and polymeric substances may provide additional agglomerative drive through Van der Waals and dipole-induced dipole interactions between the FLOPAM and organic constituents of the PFSPS explaining the greater affinity compared to the CMS system (Gregory and Barany, 2011). Though it should be noted that the non-ionic FLOPAM FA 920 SEP has demonstrated in this work an affinity for both cationic and anionic surface charge systems due to the use of hydrogen bonding making the polymer potentially versatile for nuclear decommissioning deployment.

The impact of FLOPAM dose on the flocculation of PFSPS and CMS is shown in Figs. 5A and 5B which show the cumulative percentile size distributions of PFSPS and CMS only, and the change in the volume weighted diameter ($d_{4,3}$) of the flocculated materials. The size of CMS without polymer is much larger than PFSPS as displayed in Figs. 5A, though it should be noted that the sizing techniques differ for the two materials, with FBRM and single element automated microscopy used for CMS and PFSPS respectively. However, the authors previous work has shown strong agreement between the two analytical techniques (Lockwood et al., 2021a). There is a noticeable increase in the $d_{4,3}$ for both systems with increasing polymer concentration, with the PFSPS system showing the largest relative increase in $d_{4,3}$ with lower polymer concentrations in comparison to the CMS system. This relative improvement in the size of PFSPS flocs is likely due to the greater adsorption of polymer relative to the received dose to form flocs as FLOPAM has a great affinity for the PFSPS material to facilitate flocculation compared to CMS as shown in Figs. 3A and 3B.

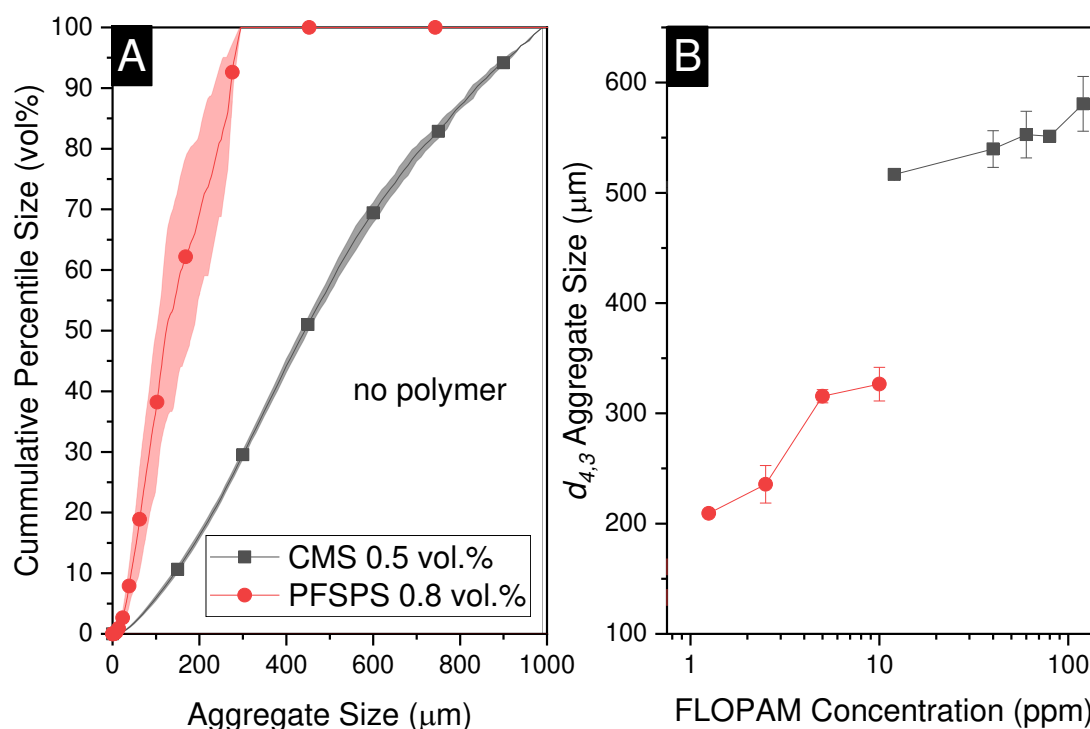


Figure 5: A) The cumulative percentile size of Pile fuel storage pond sludge (PFSPS) and Corroded Magnox Sludge (CMS) without polymer. B) The volume weighted average ($d_{4,3}$) floc diameter of flocculated PFSPS and CMS with increasing concentration of FLOPAM FA 920 SEP.

Floc size and structure is related to the sedimentation performance of the resultant flocs as density and size are parameters in all Stokes law modifications that incorporate fractal structures (Lockwood et al. 2021a, Lockwood et al, 2022; Heath et al. 2006, Vahedi and Gorczyca, 2014; Asensi and Alemany, 2022). Fig. 6A shows the relative change in zonal settling velocity as a function of FLOPAM concentration, where the presence of FLOPAM had a greater impact on the relative improvement in zonal settling rate, though overall the PFSPS system had greater settling rates by magnitude as shown in Fig. 6B. There are clear inflection points for both systems often associated with the beginning of steric stabilization (Nasser and James, 2006). The hindered settling process is complex, especially when considering fractal structures. Multivariate analysis has shown that the non-linear impact of fractal dimension of flocs is critical in determining settling rates through two mechanisms. Firstly, there is a reduction in the functional density of the aggregate by binding them to a non-symmetrical scalable geometry, i.e., fractal density decreases with increasing floc size. Secondly, functional permeability of the suspension is adjusted (the available volume of inter-particle flow paths) shown in Eqn. 1, where f_s , D_f , D_p , Φ and d_f are the functional permeability, floc diameter, primary particle diameter, solids concentration and fractal dimensions respectively. The second point should be caveated by the neglect of intra-particulate flow paths generated by increasingly porous fractal aggregates, which is not currently captured in fractal modified hindered settling models (Xiao et al.; 2013; Johnson et al.; 2016).

$$f_s = \left(1 - \Phi \left(\frac{D_f}{D_p}\right)^{3-d_f}\right)^{4.65} \quad \text{Eqn. 1}$$

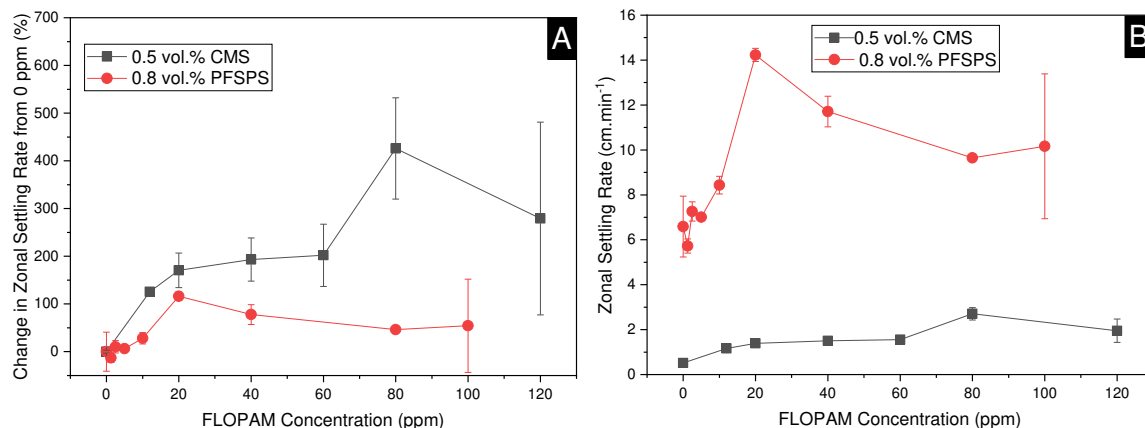


Figure 6: A) Relative change in zonal settling rates of PFSPS and CMS as a function of FLOPAM FA 920 SEP concentration. B) The absolute zonal settling rate of PFSPS and CMS as a function of FLOPAM FA 920 SEP concentrations.

Whilst the CMS aggregate is larger than PFSPS, the relatively low fractal dimension ($d_f \sim 2.07$) recorded in our previous work with similar Magnox simulants (Lockwood et al., 2021a) is lower than that for PFSPS ($d_f \sim 2.24$) (Lockwood et al.; 2022). It should be noted that attempts to record the CMS fractal dimension were not possible due to the fragile nature of flocs making them unstable when attempting to measure them by static light scattering (a consequence of the instrument dispersion unit), with CMS system responses to shear detailed in Section 5. A decrease in fractal dimension not only results in a decrease in fractal density for the individual flocs, but also decreases the functional permeability of the suspension, thus reducing the zonal settling rate of the CMS system compared to the PFSPS. Even though the system has a greater solids concentration, the non-linear influence of fractal dimension impacts the functional permeability to a greater degree, as shown in Eqn. 1. The larger floc to primary particle size ratio additionally constrains the available interparticle flow area, which may also inhibit the CMS settling ability assuming intra-particle flow is negligible.

In our previous work, another Magnox simulant, Versamag ($\text{Mg}(\text{OH})_2$) was flocculated using a statistical copolymers of polyacrylic acid and polyacrylamide in molecular percentages of 30% and 40%. Greater relative flocculation of the previous Magnox simulant was achieved compared to this work for a greater solids content (2.5 vol.%) sludges at substantially lower polymer dosages (5-20 ppm) resulting in zonal settling rates of $3 \text{ cm}\cdot\text{min}^{-1}$. The raw Versamag material was comprised of smaller constituent $\text{Mg}(\text{OH})_2$ aggregates, however, the smaller diameters and greater floc to primary particle diameters may have allowed for greater inter-particle and intra-particle flow improving the settling dynamics. This is important to consider when optimizing settling unit-operation parameters for nuclear waste consolidation against processing time. The combination of adsorption mechanisms for polyacrylamide interactions with inorganic/organic composite structure of PFSPS likely results in tighter conformation of polymer resulting in lower porosity floc structures (Gregory and Barany, 2011) and has been

observed in non-ionic polymeric flocculation of flocs in wastewater treatment (Asensi and Alemany, 2022). Whilst fractal dimension is highly influential on the behavior of zonal settling in such systems, the authors previous work has indicated that larger floc sizes are highly influential on zonal settling rate. Larger flocs encompass smaller flocs as they settle, even for systems where inter-particle distances result in a transition from creeping flow conditions to inertial flow and drag coefficients influence behavior to a greater extent (Lockwood et al. 20221a; Lockwood et al. 2022). The optimum solids concentration for such systems is a variable which should be considered during scale-up research in the future.

The other variable of interest when clarifying suspensions is the supernatant quality post-settling, especially for system burdened with colloidal materials. Fig. 7 shows the supernatant turbidity of PFSPS and CMS suspensions at 8 mins post-settling. The quality of the PFSPS liquor began at much greater turbidity compared to the CMS system. The impact of FLOPAM on the PFSPS system was highly effective at reducing the turbidity by an order of magnitude, with the turbidity inflection point coinciding with the optimum zonal settling rate performance in Figs. 6A and 6B at 10 ppm. The presence of FLOPAM had little impact on the supernatant liquor quality of the CMS system where the turbidity began to increase when approaching the optimum settling rate (80 ppm) and continued to rise beyond this point. This turbidity increase is typically indicative of steric stabilization at FLOPAM concentrations 25% above the optimum settling concentration resulting in nearly four times greater turbidity than without polymer addition (Nasser and James, 2006). Whereas the PFSPS system saw small relative increases in turbidity at 1000% the optimum dose concentration and still maintaining an order of magnitude lower turbidity. This is important in nuclear decommissioning operations as the PFSPS system has demonstrated greater resilience to overdosing than the CMS system meaning more flexibility on process control designs.

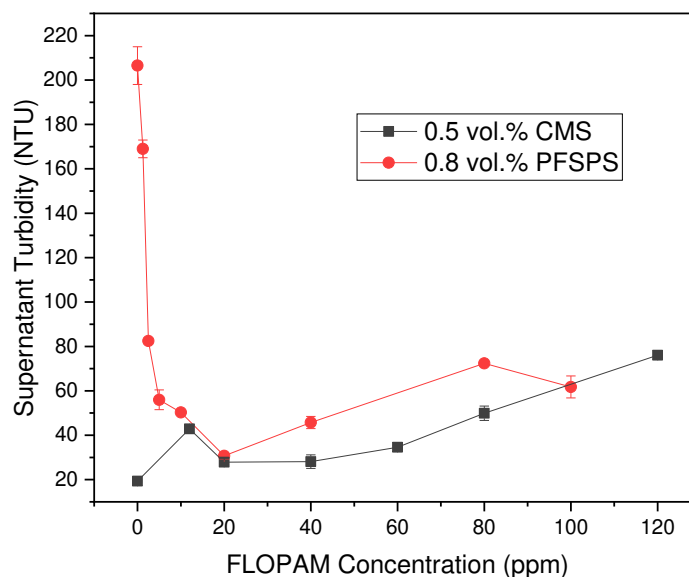


Figure 7: The supernatant turbidity of Pile fuel storage pond sludge and corroded Magnox sludge after 10 minutes of settling.

5. ENGINEERING RESEARCH CONSIDERATIONS

Scaling up the use of polymers from bench scale tests to deployment requires consideration of practical challenges on site. These include:

- The impact of variable solution chemistry
- The deployment methodology impact of shear on process for mobilization

During decommissioning operations, the solution chemistry of cooling waters could vary for a range of reasons. Understanding the impact of electrolyte concentrations on the flocculation ability of FLOPAM is key from a deployment perspective, potentially requiring alteration to dosing regimens depending on the electrolyte presence in the carrier fluid of suspensions. An investigation into the impact of electrolytes on the performance of CMS flocculated with FLOPAM in a range of saline conditions was conducted and found that even low concentrations of polymer could affect the adsorption of polymer to CMS and drastically affect the zonal settling rate. Fig. 8A shows the impact on the remaining FLOPAM in the supernatant liquor, where even low concentrations have a significant impact on zonal settling rate, and approaching 1 M NaCl, leads to negligible difference compared to the raw unflocculated CMS material. The adsorption decrease can be observed at conditions as low as 10 mM also, where the remaining FLOPAM in the supernatant liquor increases with increasing concentrations. This effect could be due to a decrease in the solubility of the FLOPAM, as well as Debye screening between its amide functional groups and the hydroxyl surface species of the CMS (Gregory and Barany, 2011). Further work is required to identify the impact of electrolytes on PFSPS flocculation process.

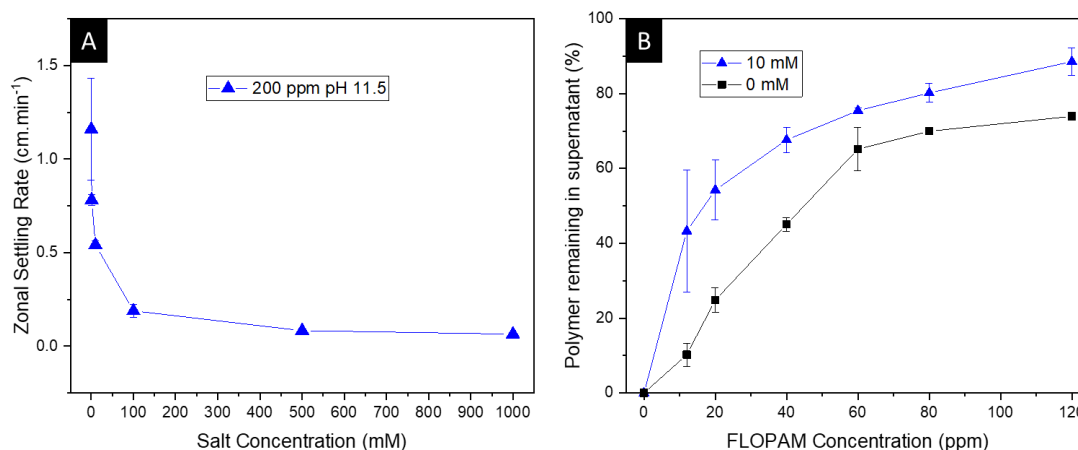


Figure 8: A) The change in zonal settling velocity of 1.25 vol.% corroded Magnox sludge flocculated with 200 ppm FLOPAM FA 920 SEP with increasing concentrations of NaCl. B) The change in FLOPAM FA 920 SEP concentration remaining in supernatant liquor after contacting with 0.5 vol.% corroded Magnox Sludge with increasing FLOPAM FA 920 SEP dose.

Given the sensitivity to electrolyte concentration, the corresponding question is how does one deploy such a reagent into legacy facilities at the Sellafield site? This is a highly constrained problem with little opportunity to retrofit process equipment into such facilities (Hastings et al., 2007; Arnold, 2007). Additionally, it is known that shear has impact on the flocculation process (Vajihinejad and Soares, 2018). However, the CMS material has demonstrated non-

conventional flocculation behavior compared to the PFSPS material. After inversion of the settling cylinder, the PFSPS material settles instantaneously, achieving visibly clearer supernatant liquors within 2 minutes for doses of 10 ppm for a 0.8 vol.% suspension of PFSPS shown in Fig. 9A. However, the CMS material has a destabilization period as demonstrated in Fig. 9B. before flocculation becomes visibly present. Further investigation into the shear response properties of CMS found that by varying the shear rate from 300 rpm to 50 rpm incrementally then back to 300 rpm and down to 50 rpm, again the volume weighted average chord length of the flocculated CMS material begins to increase as shear decrease shown in Fig. 9C. Then upon increasing the shear rate to 300 rpm, the flocs breakdown again but recover as shear is removed from the system. This pseudo-thixotropic behavior was observed practically by compared two flocculated samples of CMS over a period of three weeks, where once sample was kept on a bench top and one sample was place on a carousel stirrer at 2 rpm. The floc size distribution was compared for the two systems and found that the stationary sample had greater floc sizes than the carousel sample shown in Fig. 9D. Indicating fragility in the floc system requiring near transient conditions to facilitate flocculation. From the optics of deployment, this behavior is potentially a ‘double-edged sword’, where for processes such as filtration, a flocculated CMS system would, in theory, behave poorly, breaking up during transport to a filter or upon impact with the membrane for example which is often required in dewatering processes and would not be advantageous (Hastings, et al., 2007). However, this break down and recovery could also be theoretically advantageous, as the system will likely have lower critical deposition velocity in a sheared state but then flocculate in holding tanks and settling efficiently. Future work should further probe the impact of shear on the PFSPS system.

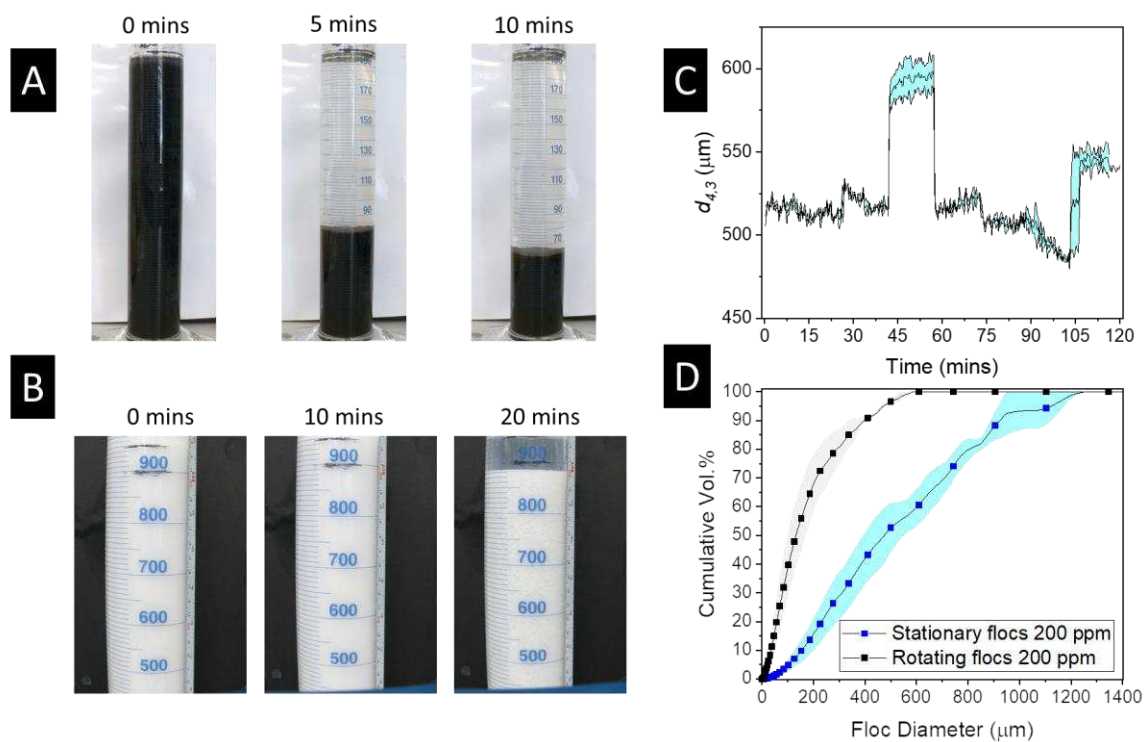


Figure 9: A) Images of 0.8 vol.% Pile fuel storage pond sludge flocculated with 10 ppm FLOPAM FA 920 SEP at 0, 5 and 10 minutes show instantaneous response to polymer dose. B) 1.25 vol.% corroded Magnox sludge flocculated with 200 ppm FLOPAM FA 920 SEP at 0,

10 and 20 minutes showing destabilization period before flocculation and settling. C) the $d_{4,3}$ chord length distribution response to varying impeller speeds of corroded Magnox sludge flocculated with 200 ppm of FLOPAM FA 920 SEP with a 1 mM NaCl electrolyte background. D) The cumulative frequency floc size distributions of corroded Magnox sludge flocculated with 200 ppm FLOPAM FA 920 SEP left on a benchtop for 3 weeks vs a carousel stirrer at 2 rpm.

6. CONCLUSIONS

In this study, a polyacrylamide-based non-ionic polymer displayed versatile performance in flocculating both cationic and anionic surface speciated corroded Magnox sludge and Pile fuel storage pond sludge respectively to differing degrees. For both systems, there was a marked improvement in performance especially considering zonal settling rates, which could reduce settling vessel residence times and increase the paste of sludge removal from legacy ponds and silos. The differing surface speciation and nature of the materials proved important when considering the affinity of the polymer for the particle surface and should be the first consideration when assessing the viability of polymers to remove slow settling particles and colloidal material in nuclear decommissioning operations. Whilst literature has shown more tailored functional groups in polymeric flocculants can improve performance for the material observed in this work (Lockwood et al., 2021a; Roselet et al., 2015), resistance to electrolyte concentrations is important, with even non-ionic polymers showing vulnerability in brackish and saline conditions. Furthermore, the two systems showed varying resistance to shear conditions and this should also be considered for any future deployment of polymers onto other nuclear materials. Such shear dependent behavior will likely affect rheology and transport properties of the materials, though these changes may also be advantageous in some scenarios.

7. REFERENCES

- Arnold, L. Windscale 1957: *Anatomy of a Nuclear Accident*; Palgrave Macmillan, 2007.
- Barlow, S, T. Fisher, A, J. Bailey, D, J. Blackburn, L, R. Stennett, M, C. Hand, R, J. Morgan, S, P. Hyatt, N, C. Corkhill, C, L. Thermal Treatment of nuclear fuel-containing Magnox sludge radioactive waste. *Journal of Nuclear Materials*. 2021, **552**, 152965.
- de Martín, L. Fabre, A. Ruud van Ommen, J. The Fractal Scaling of Fluidized Nanoparticle Agglomerates. *Chem. Eng. Sci.* 2014, **112**, 79–86.
- Dyer, A. Hriljac, J. evans, N. Stokes, I. rand, P. Kellet, S. Harjula, R. Moller, T. Maher, Z. Heatlie-Branson, R. Austin, J. Williamson-Owens, S. Higgins-Bos, M. Smith, K. O'Brien, L. Smith, N. Bryan, N. The use of columns of the zeolite clinoptilolite in the remediation of aqueous nuclear waste streams. *Journal of Radioanalytical and Nuclear Chemistry*. 2018, **318**, 2473-2491.
- Gregory, J. Barany, S. Adsorption and flocculation by polymers and polymer mixtures. *Advances in Colloid and Interface Science*. 2011, 169(1), 1-12.
- Gregory, K, P. Elliot, G, R. Robertson, H. Kumar, A. Wanless, E, J. Webber, G, B. Craig, V, S, J. Andersson, G, G. Page, A, J. Understanding specific ion effects and the Hofmeister series. *Phys. Chem. Chem. Phys.* 2022, **24**, 12682-12718

Gregson, C, R. Goddard, D, T. Sarsfield, M, J. Taylor, R, J. Combined electron microscopy and vibrational spectroscopy study of corroded Magnox sludge from a legacy spent nuclear fuel storage pond. *Journal of Nuclear Materials*. 2011, **1**(1), 145-156.

Hallam, K, R. Minshall, P, C. Heard, P, J. Flewitt, P, E, J. Corrosion of the alloys Magnox AL80, Magnox ZR55 and pure magnesium in air containing water vapour. *Corrosion Science*. 2016, **112**, 347-363.

Hastings, J. J. Rhodes, D. Fellerman, A, S. Mckendrick, D. Dixon, C. New Approaches for Sludge Management in the Nuclear Industry. *Powder Technol*. 2007, **174** (1–2), 18–24.

Heath, A, R. Bahri, P, A. Fawell, P, D. Farrow, J, B. Polymer flocculation of calcite: relating aggregate size to settling rate. *AIChEJ*. 2006, **52**(6), 1987-1994.

Hope, J, A. Malarkey, J. Baas, J, H. Peakall, J. Parsons, D, R. Manning, A, J. Bass, S, J. Litchman, I, D. Thorne, P, D. Ye, L. Paterson, D, M. Interactions between sediment microbial ecology and physical dynamics drive heterogeneity in contextually similar depositional systems. *Limnology and Oceanography*. 2020, **65**, 2403-2419.

Jackson, S, F. Monk, S, D. Riaz, Z. An Investigation towards Real Time Dose Rate Monitoring, and Fuel Rod Detection in a First-Generation Magnox Storage Pond (FGMSP). *Appl. Radiat. Isot*. 2014, **94**, 254–259.

Johnson, M, J. Peakall, J. Fairweather, M. Biggs, S. Harbottle, D. Hunter, T.N. Characterisation of multiple hindered settling regimes in aggregated mineral suspensions. *I&EC Res*. 2016, **55**, 9983-9993.

Ji. Y. Lu, Q., Liu, Q.Zeng, H. effect of solution salinity on settling of mineral tailings by polymer flocculants. *Colloids and surfaces A: Physiochemical and Engineering Aspects*. 2013. **430**, 29-38.

Koutsopouloua, E. Papoulisa, D. Tsolis-Katagasa, P. Kornarosb, M. Clay minerals used in sanitary landfills for the retention of organic and inorganic pollutants. *Applied Clay Science*. 2010, **49**(4), 372-382.

Levitt, D, B. Pope, G, A. Jouenne, S. Chemical degradation of polyacrylamide polymers under alkaline conditions. *SPE Res Eval & Eng*. 2011, **14** (03), 281-286.

Lockwood, A, P, G. Peakall, J. Warren, N, J. Randall, G. Barnes, M. Harbottle, D. Hunter, T, N. Structure and sedimentation characterisation of sheared Mg(OH)₂ suspensions flocculated with anionic polymers. *Chem Eng Sci*, 2021a, **231**, 116274.

Lockwood, A, P, G. Kok Shun, P. Peakall, J. Warren, N, J. Barber, T. Basharat, N. Randall, G. Barnes, M, G. Harbottle, D. Hunter, T, N. Flotation using sodium dodecyl sulphate and sodium lauryl isethionate for rapid dewatering of Mg(OH)₂ suspensions. *RSC Advances*. 2021b, **11**, 18661.

Lockwood, A, P, G. Rumney, J, R, L. Barnes, M, G. Dodds, J, M. Peakall, J. Hunter, T, N. Approximation of hindered zonal settling rates for flocculated inorganic/organic composite suspensions in inertial flow conditions. *J. Water Proc. Engr.* 2023, **51**, 103459.

Maher, Z. Ivanov, P. O'Brien, Sims, H. Taylor, R, J. Heath, S, L. Livens, F, R. Goddard, D. Kellet, S. Rand, P. Bryan, N, D. Americium and plutonium association with magnesium hydroxide colloids in alkaline nuclear industry process environments. *Journal of Nuclear Materials.* 2016, **468**, 84-96.

Mignacca, B. Locatelli, G. Sainati, T. Deeds not words: Barriers and Remedies for Small Modular nuclear Reactors. *Energy.* 2020, **206**, 118137.

Nasser, M, S. James, A, E. The effect of polyacrylamide charge density and molecular weight on the flocculation and sedimentation behaviour of kaolinite suspensions. *Separation and Purification Technology*, 2006, **52**, 2, 241-252.

Nyysola, A. Ahlgren, J. Microbial degradation of polyacrylamide and the deamination product polyacrylate. *International biodeterioration & Biodegradation.* 2019, **139**, 24-33

O'Shea, J. P. Qiao, G. G. Franks, G. V. Solid-Liquid Separations with a Temperature-Responsive Polymeric Flocculant: Effect of Temperature and Molecular Weight on Polymer Adsorption and Deposition. *J. Colloid Interface Sci.* 2010, **348**(1), 9–23.

Prajitno, M, Y. Tangparitkul, S. Zhang, H. Harbottle, D. Hunter, T, N. The effect of cationic surfactants on improving natural clinoptilolite for the flotation of cesium. *Journal of Hazardous Materials.* 2021, **402**, 123567.

Roselet, F. Vandamme, D. Roselet, M. Muylaert, K. Abreu, P, C. Screening of commercial natural and synthetic cationic polymers for flocculation of freshwater and marine microalgae and effects of molecular weight and charge density. *Algal Research*, 2015, **10**, 183-188.

Rosenqvist, J. Peraan, P. Sjoberg, S. Protonation and charging of nanosized gibbsite (α -Al(OH)₃) particles in aqueous suspension. *Langmuir.* 2002, **18**(12) 4598-4604.

Sabbagh, F. Khatir, N, M. Karim, A, K. Omidvar, A. Nazari, Z. Jaber, R. Mechanical Properties and Swelling Behavior of Acrylamide Hydrogels using Montmorillonite and Kaolinite as Clays. *Journal of environmental treatment techniques.* 2019, **7**(2) 211-219.

Sung Ng, W.; Connal, L. A.; Forbes, E.; Mohanaragam, K.; Franks, G. V. In Situ Study of Aggregate Sizes Formed in Chalcopyrite-Quartz Mixture Using Temperature-Responsive Polymers. *Adv. Powder Technol.* 2018, **29**(8), 1940–1949.

Vahedi, A. Gorczyca, B. Settling velocities of multifractal flocs formed in chemical coagulation process. *Water Res.*, 2014, **53**, 322-328.

Vajihinejad, V. Soares, J. B. P. Monitoring Polymer Flocculation in Oil Sands Tailings: A Population Balance Model Approach. *Chem. Eng. J.* 2018, **346**, 447–457.

Wierenga, A, M. Lenstra, T, A, J. Philipse, A, P. Aqueous dispersions of colloidal gibbsite platelet: synthesis, characterisation and intrinsic viscosity measurements. *Colloids and Surfaces A*. 1998, **134**, 359-371.

Woodall, S, D. Hambley, M. Rawcliffe, J. Wiley, D. Hambley, D. Characterisation of corrosion products from degraded uranium dioxide fuel. *Journal of Nuclear Materials*. 2021. **552**, 152986.

Xiao, F. Lam, K, M. Li, X. Investigation and visualization of internal flow through particle aggregates and microbial flocs using particle image velocimetry. *J. Colloid Interface Sci.*, 2013, **397**, 163-168

8. ACKNOWLEDGEMENTS

The authors would like to thank Sellafield Ltd. for primary funding. TH also acknowledges further funding from the Engineering and Physical Sciences Research Council (EPSRC) through the U.K. TRANSCEND (Transformative Science and Engineering for Nuclear Decommissioning) project (Grant No. EP/S01019X/1). Thanks are also given to Stuart Micklethwaite and the Leeds Electron Microscopy and Spectroscopy (LEMAS) Centre for their assistance and guidance with the cryogenic scanning electron microscope experiments and Rachel Gasior and the University of Leeds School of Geography for their assistance with total organic carbon measurements.